Research article

JHEP|Reports

Pathological bile acid concentrations in chronic cholestasis cause adipose mitochondrial defects

Authors

Weinan Zhou, Philip VanDuyne, Chi Zhang, Yushan Liu, Ryan Riessen, Maribel Barragan, Blair M. Rowitz, Margarita Teran-Garcia, Stephen A. Boppart, Sayeepriyadarshini Anakk

Correspondence

anakk@illinois.edu (S. Anakk).

Graphical abstract

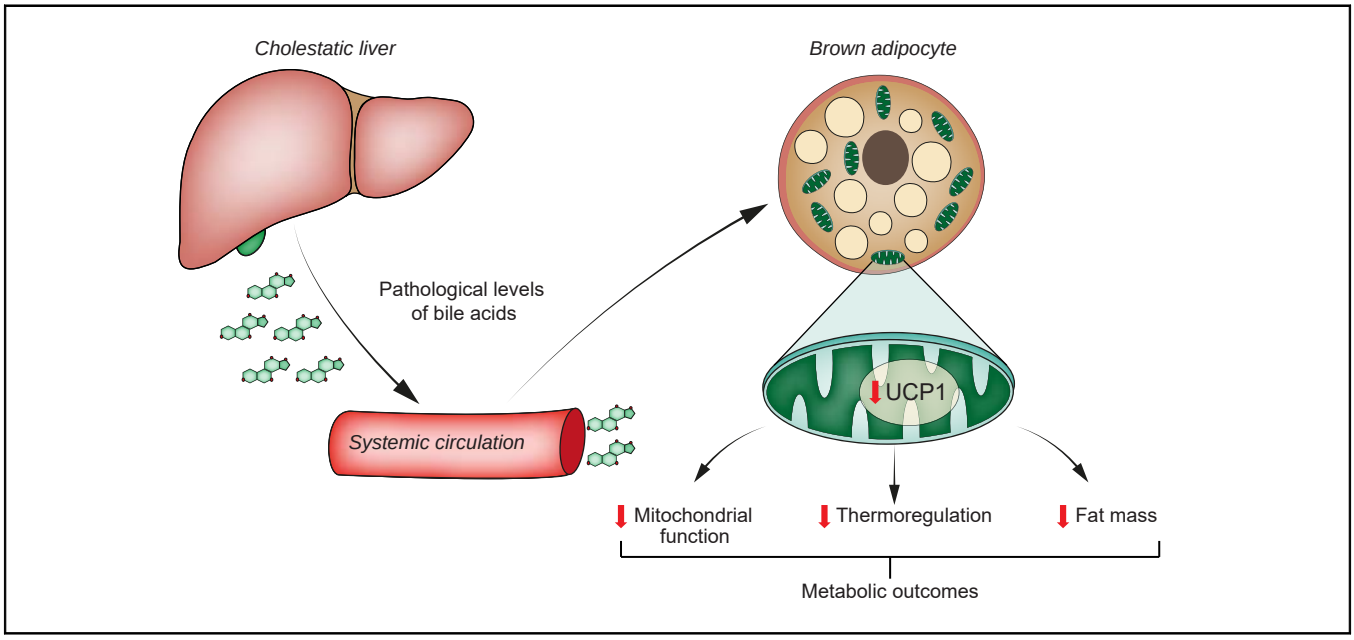

Highlights

- Cholestasis impairs brown fat mitochondrial function and thermogenesis.
- Under thermoneutral housing, control brown fat mimics the cholestatic brown fat.
- UCP1 activation restores expression of thermogenic genes reduced by bile acid excess.

Impact and Implications

We uncover a detrimental effect of chronic bile acid overload on adipose mitochondrial function. Pathological concentration of different BAs reduces the expression of distinct genes involved in energy expenditure, which can be mitigated with pharmacological UCP1 activation.

https://doi.org/10.1016/j.jhepr.2023.100714

Research article

JHEP|Reports

Pathological bile acid concentrations in chronic cholestasis cause adipose mitochondrial defects

Weinan Zhou,[1] Philip VanDuyne,[1] Chi Zhang,[2] Yushan Liu,[1] Ryan Riessen,[1] Maribel Barragan,[3] Blair M. Rowitz,[4,5] Margarita Teran-Garcia,[3,5] Stephen A. Boppart,[2,5,6,7,8] Sayeepriyadarshini Anakk[1,2,3,8,*]

[1]*Department of Molecular and Integrative Physiology, University of Illinois Urbana-Champaign, Urbana, IL, USA;* [2]*Beckman Institute for Advanced Science and Technology, University of Illinois Urbana-Champaign, Urbana, IL, USA;* [3]*Division of Nutritional Sciences, University of Illinois Urbana-Champaign, Urbana, IL, USA;* [4]*Carle Foundation Hospital, Urbana, IL, USA;* [5]*Carle Illinois College of Medicine, University of Illinois Urbana-Champaign, Urbana, IL, USA;* [6]*Department of Bioengineering, University of Illinois Urbana-Champaign, Urbana, IL, USA;* [7]*Department of Electrical and Computer Engineering, University of Illinois Urbana-Champaign, Urbana, IL, USA;* [8]*Cancer Center at Illinois, University of Illinois Urbana-Champaign, Urbana, IL, USA*

JHEP Reports **2023.** https://doi.org/10.1016/j.jhepr.2023.100714

Background & Aims: Although fat loss is observed in patients with cholestasis, how chronically elevated bile acids (BAs) impact white and brown fat depots remains obscure.
Methods: To determine the direct effect of pathological levels of BAs on lipid accumulation and mitochondrial function, primary white and brown adipocyte cultures along with fat depots from two separate mouse models of cholestatic liver diseases, namely (i) genetic deletion of farnesoid X receptor (*Fxr*); small heterodimer (*Shp*) double knockout (DKO) and (ii) injury by 3,5-diethoxycarbonyl-1,4-dihydrocollidine (DDC), were used.
Results: As expected, cholestatic mice accumulate high systemic BA levels and exhibit fat loss. Here, we demonstrate that chronic exposure to pathological BA levels results in mitochondrial dysfunction and defective thermogenesis. Consistently, both DKO and DDC-fed mice exhibit lower body temperature. Importantly, thermoneutral (30 °C) housing of the cholestatic DKO mice rescues the decrease in brown fat mass, and the expression of genes responsible for lipogenesis and regulation of mitochondrial function. To overcome systemic effects, primary adipocyte cultures were treated with pathological BA concentrations. Mitochondrial permeability and respiration analysis revealed that BA overload is sufficient to reduce mitochondrial function in primary adipocytes, which is not as a result of cytotoxicity. Instead, we found robust reductions in uncoupling protein 1 (*Ucp1*), PR domain containing 16 (*Prdm16*), and deiodinase, iodothyronine, type II (*Dio2*) transcripts in brown adipocytes upon treatment with chenodeoxycholic acid, whereas taurocholic acid led to the suppression of *Dio2* transcript. This BA-mediated decrease in transcripts was alleviated by pharmacological activation of UCP1.
Conclusions: High concentrations of BAs cause defective thermogenesis by reducing the expression of crucial regulators of mitochondrial function, including UCP1, which may explain the clinical features of hypothermia and fat loss observed in patients with cholestatic liver diseases.
Impact and Implications: We uncover a detrimental effect of chronic bile acid overload on adipose mitochondrial function. Pathological concentration of different BAs reduces the expression of distinct genes involved in energy expenditure, which can be mitigated with pharmacological UCP1 activation.

Introduction

Patients with liver diseases display increased systemic bile acid (BA) levels up to several hundred micromolar (∼300 μM) compared to healthy individuals.[1] Further, a wide range of cholestatic liver diseases, including progressive familial intrahepatic cholestasis,[2] primary biliary cholangitis,[3] primary sclerosing cholangitis,[4] and intrahepatic cholestasis of pregnancy,[5] display loss of body weight and fat mass. These findings indicate that serum BAs are linked with energy metabolism. Previous studies reveal that treating with low BA concentrations can promote heat production in the brown adipose tissue (BAT) and increase energy expenditure by activating membrane G protein-coupled receptor TGR5.[6,7] However, the consequence of prolonged and persistent exposure to pathological BA levels on the adipose tissue is yet to be delineated.

Because excessive BAs during cholestasis are known to cause mitochondrial defect in the liver[8,9] and suppress fatty acid oxidation and peroxisome proliferative activated receptor, gamma, coactivator 1 alpha (*Pgc1a*) expression in the heart[10,11] in a dose-dependent manner, we investigated whether chronically elevated levels of BAs impact mitochondrial function in the adipose tissue. We examined both BAT, which is linked to fat burning and is rich in mitochondria, and white adipose tissue (WAT), which is primarily responsible for fat storage.[12]

Keywords: Bile acid; Cholestasis; Adipose tissue; Mitochondrial function.
Received 22 July 2022; received in revised form 13 January 2023; accepted 4 February 2023; available online 23 February 2023
* Corresponding author. Address: Department of Molecular and Integrative Physiology, University of Illinois Urbana-Champaign, Urbana, IL 61801, USA. Tel.: +1 217 300 7905; fax: +1 217 244 5858
E-mail address: anakk@illinois.edu (S. Anakk).

We first measured thermogenic gene expression in the BAT from mice after short-term exposure to cholic acid (CA)-enriched diet.[13] Next, we examined the adipose histology and mitochondrial structure with electron microscopy in the genetic mouse model for juvenile onset cholestasis (farnesoid X receptor [*Fxr*]; small heterodimer [*Shp*] double knockout [DKO]).[11,14–16] Then, we determined whether we could overcome the brown fat defect by housing the mice in thermoneutral conditions. To validate this finding, we investigated whether another model of cholestasis, which is caused by chronic exposure of wild-type (WT) mice to 3,5-diethoxycarbonyl-1,4-dihydrocollidine (DDC) diet,[17] also led to compromised adipose mitochondrial function. Adipose depots from both models of cholestasis were analysed for mitochondrial respiration, enzyme activity, mitochondrial DNA (mtDNA) copy number, and gene expression. We also challenged the WT and DKO mice with a high-fat diet (HFD) to test whether elevated BAs contribute to fat loss as well as thermogenic defect during obesity. We then investigated a cell autonomous role for BAs in the adipose milieu using differentiated primary adipocyte cultures from both fat depots *in vitro* and analysed mitochondrial membrane potential, respiration, and gene expression in the presence and absence of BA overload. Finally, we tested whether a pharmacological activator of uncoupling protein 1 (UCP1) can restore thermogenic gene expression pattern in the adipocytes.

Materials and methods

Human adipose tissue

Human perigastric WAT samples were obtained from tissue normally discarded from obese patients undergoing Roux-en-Y gastric bypass surgery.[18] All procedures were approved by the institutional review board (IRB) at Carle Foundation Hospital and the University of Illinois Urban-Champaign (IRB protocol # 14092). Informed consent was obtained from the participants, and the privacy rights of the participants were observed.

Animals

To induce short-term BA overload, 8- to 10-week-old male C57BL/6 WT mice were fed with 1% CA-supplemented (Envigo, Indianapolis, IN, USA) or normal chow (Envigo) diet for 5 days.[13] The generation of DKO mice has been described.[14] Male DKO and WT mice (8 to 10 weeks old) were used. These mice were bred and maintained on a 12:12 h light/dark cycle with *ad libitum* access to tap water and a normal chow diet in a climate-controlled (23 °C) animal facility at the University of Illinois Urbana-Champaign. At 8–10 weeks, mice were fed a normal chow or 45% HFD (Envigo) for 8 weeks to mimic obesogenic conditions and housed either at room temperature (RT; 23 °C) or at thermoneutrality (TN; 30 °C) to blunt brown fat thermogenic activity.[19] To induce chronic cholestatic liver disease, 8- to 10-week-old male WT mice were fed with 0.1% DDC-supplemented (Envigo) or normal chow diet for 6 weeks.[17]

DKO and WT mice were weighed weekly. After 8-week chow or 45% HFD feeding, a subset of the mice was used for monitoring core body temperature fluctuation using a Comprehensive Laboratory Animal Monitoring System (CLAMS) (Oxymax, Columbus Instruments, Columbus, OH, USA). Briefly, animals were surgically implanted with a transmitter in the abdominal cavity and acclimated to the CLAMS cages. Fluctuations in the body temperature were recorded over the subsequent 24-h period. Mice

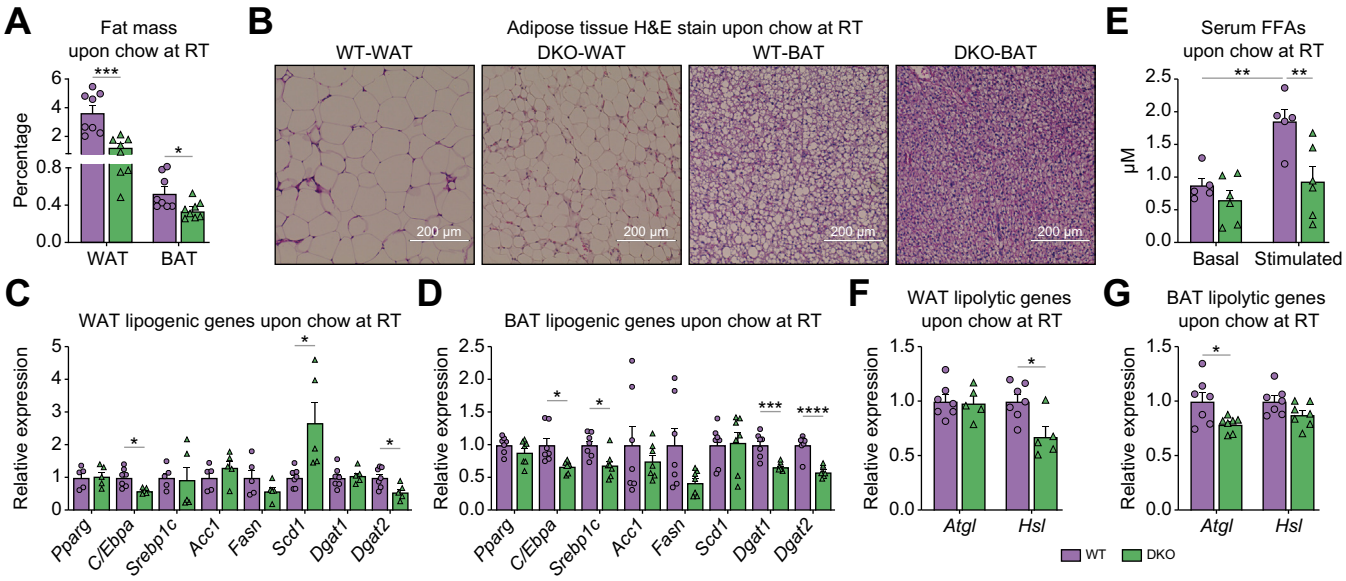

Fig. 1. Cholestatic DKO mice display decreased fat accumulation. DKO and WT mice were fed with chow and housed at RT. (A–D) Fat mass/body weight ratios (n = 8 mice) (A), representative images of H&E-stained WAT and BAT sections (scale bar: 200 µm; n = 6–7 mice) (B), and mRNA levels of genes related to lipogenesis in the WAT (C) and BAT (D) from DKO and WT mice (n = 5–7 mice). (E–G) Levels of serum FFAs under basal and isoproterenol-stimulated conditions (n = 5–6 mice) (E), and mRNA levels of lipolytic genes in the WAT (F) and BAT (G) from DKO and WT mice (n = 5–7 mice). Data are represented as mean ± SEM. Differences between two groups were analysed using Student's *t* test, and multiple-group comparisons were analysed using a two-way ANOVA with a Fisher's LSD *post hoc* test. $^{*}p$ <0.05, $^{**}p$ <0.01, $^{***}p$ <0.001, $^{****}p$ <0.0001. *Acc1*, acetyl-CoA carboxylase 1; *Atgl*, adipose triglyceride lipase; BAT, brown adipose tissue; *C/Ebpa*, CCAAT/enhancer binding protein alpha; *Dgat1*, diacylglycerol O-acyltransferase 1; *Dgat2*, diacylglycerol O-acyltransferase 2; DKO, *Fxr* and *Shp* double knockout; *Fasn*, fatty acid synthase; FFA, free fatty acid; *Fxr*, farnesoid X receptor; *Hsl*, hormone-sensitive lipase; H&E, hematoxylin and eosin; LSD, least significant difference; *Pparg*, peroxisome proliferator activated receptor gamma; RT, room temperature; *Scd1*, stearoyl-coenzyme A desaturase 1; *Shp*, small heterodimer; *Srebp1c*, sterol regulatory element binding protein 1c; WAT, white adipose tissue; WT, wild-type.

were sacrificed at the end of the experimental regimen. Interscapular BAT, inguinal WAT, and gonadal WAT were collected for primary preadipocyte culture and for the analysis of histology, gene expression, protein levels, the degree of lipid unsaturation, mitochondrial respiratory enzyme activity, and isolated mitochondrial respiration.

DDC- and chow-fed WT mice were weighed weekly. After 6 weeks, a subset of mice was used for indirect calorimetry using the CLAMS as previously described.[16] Body surface temperature in the perianal region was measured using a non-contact infrared thermometer.[20] Mice were sacrificed at the end of the experimental regimen. Serum, liver, interscapular BAT, and gonadal WAT were collected for analysis of total BA levels, histology, gene expression, and to isolate mitochondria and perform respiration assays. All experiments were performed following the National Institutes of Health guidelines for the care and use of laboratory animals, and all procedures were approved by the Institutional Animal Care and Use Committee at the University of Illinois Urbana-Champaign.

Statistical analysis

Data were expressed as means ± SEM. Statistical analyses were performed using GraphPad Prism 9 software (GraphPad Software Inc., San Diego, CA, USA). Differences between two groups were analysed using Student's *t* test, and multiple-group comparisons were analysed using a one-way or two-way ANOVA with a Fisher's least significant difference (LSD) *post hoc* test. A value of $p < 0.05$ was considered statistically significant.

For further details regarding the materials and methods used, please refer to the Supplementary CTAT Table and Supplementary information.

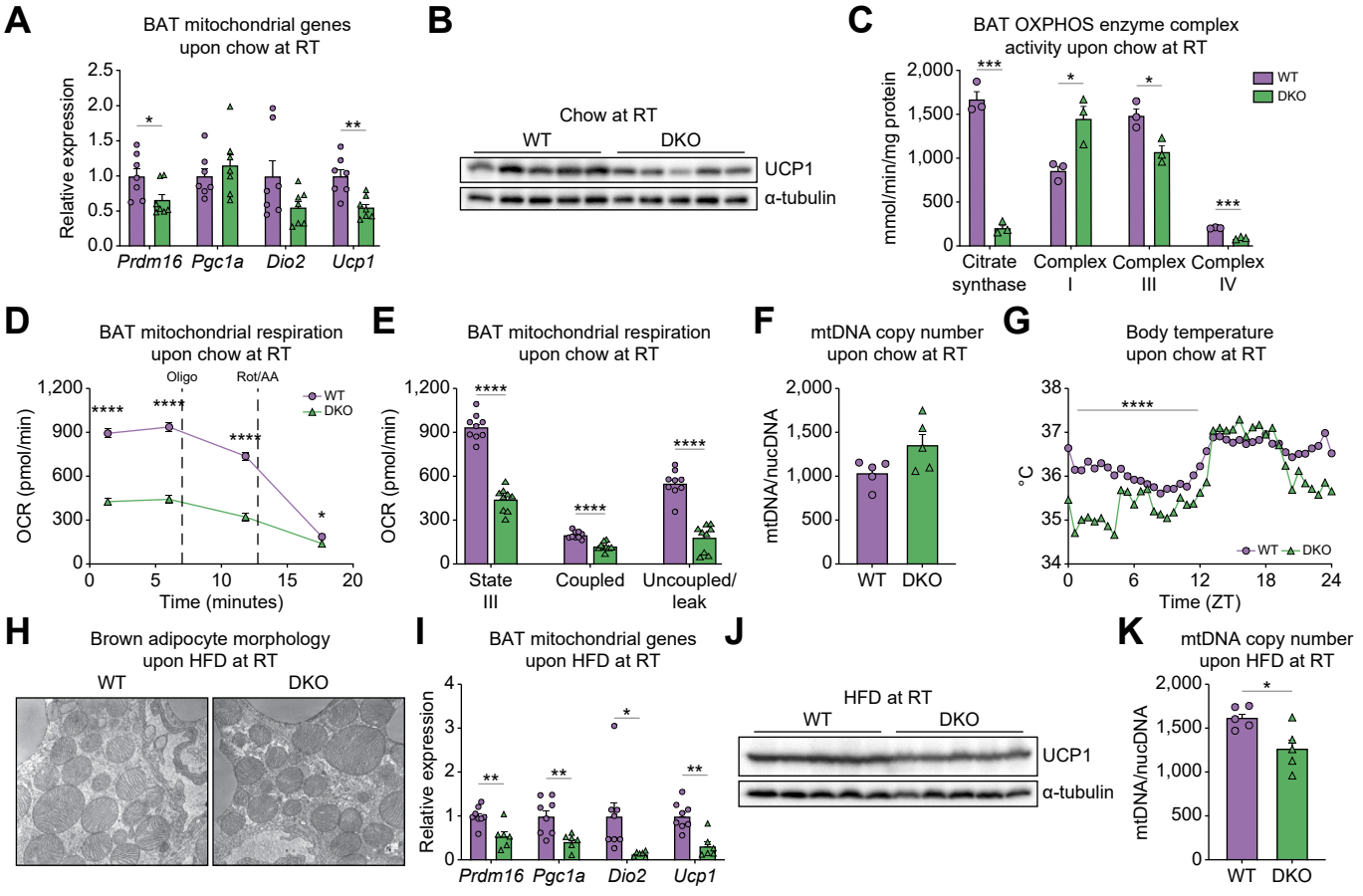

Fig. 2. Cholestatic DKO mice exhibit BAT mitochondrial dysfunction. DKO and WT mice were fed with chow or HFD for 8 weeks and housed at RT. (A–E) mRNA levels of thermogenic genes (n = 7 mice) (A), protein levels of UCP1 (n = 5 mice) (B), and the activities of OXPHOS enzyme complexes (n = 3 mice) (C), and traces (D) and quantification (E) of OCR of isolated mitochondria of the BAT from WT and DKO mice upon chow. OCR at state III and in the presence of Oligo or Rot/AA (n = 9 wells per group isolated from BAT of 5 mice). (F) mtDNA copy number of BAT from WT and DKO mice upon chow (n = 5 mice). (G) Body temperature of DKO and WT mice for 24 h upon chow (n = 7 mice). (H) Representative electron microscopy images (magnification: 10,000 ×) from DKO and WT mice upon HFD (n = 3–4 mice). (I–K) mRNA levels of thermogenic genes (n = 6–8 mice) (I), protein levels of UCP1 (n = 5 mice) (J), and mtDNA copy number (n = 5 mice) (K) of BAT from DKO and WT mice at RT upon HFD. Data are represented as mean ± SEM (A, C–F, I, and K) or mean (G). Differences between two groups were analysed using Student's *t* test, and multiple-group comparisons were analysed using a two-way ANOVA with a Fisher's LSD *post hoc* test. *$p < 0.05$, **$p < 0.01$, ***$p < 0.001$, ****$p < 0.0001$. BAT, brown adipose tissue; *Dio2*, deiodinase, iodothyronine, type II; DKO, *Fxr* and *Shp* double knockout; *Fxr*, farnesoid X receptor; HFD, high-fat diet; LSD, least significant difference; mtDNA, mitochondrial DNA; nucDNA, nuclear DNA; OCR, oxygen consumption rate; Oligo, oligomycin; OXPHOS, oxidative phosphorylation; *Pgc1a*, peroxisome proliferative activated receptor, gamma, coactivator 1 alpha; *Prdm16*, PR domain containing 16; Rot/AA, rotenone and antimycin A; RT, room temperature; *Shp*, small heterodimer; *Ucp1*, uncoupling protein 1; WT, wild-type; ZT, zeitgeber time.

Results

Chronic BA excess in DKO mice results in compromised brown adipose function

Previously, a 0.5% CA diet had been shown to promote the expression of thermogenic genes *Pgc1a* and deiodinase iodothyronine type II (*Dio2*), indicating the beneficial effect of low dose of BAs.[6] We performed a short-term exposure to 1% CA diet[13] and found that we were able to recapitulate this increase in *Dio2* and *Pgc1a* in BAT (Fig. S1). We then examined the DKO mouse model of juvenile onset cholestasis[11,14–16] to study the effect of chronic BA overload on the adipose tissue. As previously shown, DKO mice display excessive BA concentrations in the serum (Fig. S2A)[14,15] and exhibit lower body weight and resistance to fatty liver disease.[16] Even under chow diet, these mice displayed reduced white and brown fat mass (Fig. 1A) with smaller adipocyte size (Fig. 1B and Fig. S2B) compared with WT mice. These findings correlated well with reduced expression of lipogenic genes in the WAT (CCAAT/enhancer binding protein

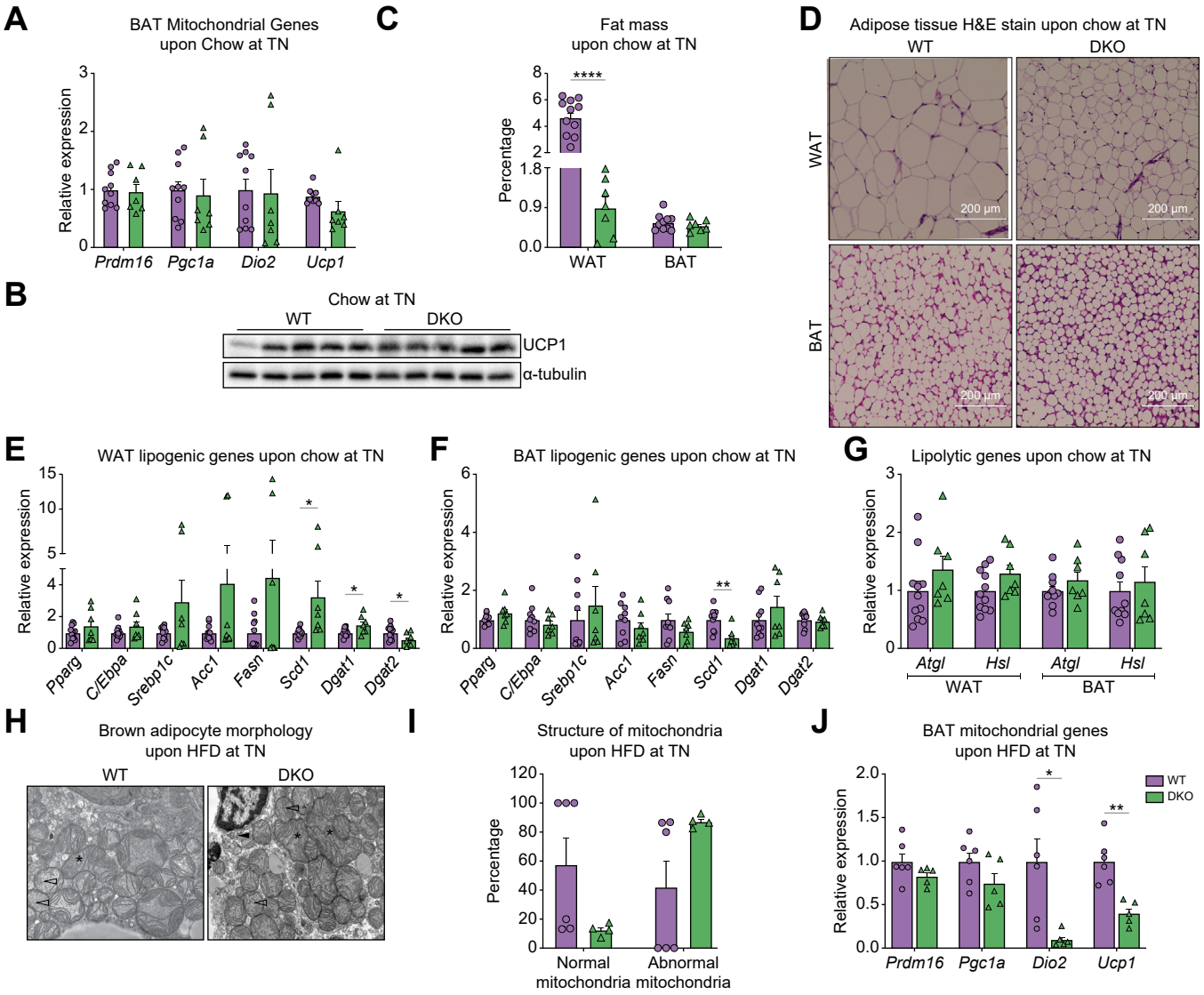

Fig. 3. Thermoneutral housing replicates the brown fat phenotype of cholestatic DKO in the WT mice. DKO and WT mice were fed with chow or HFD for 8 weeks and housed at TN. (A,B) mRNA levels of thermogenic genes (n = 7–10 mice) (A) and protein levels of UCP1 (n = 5 mice) (B) of the BAT from WT and DKO mice upon chow. (C–H) Fat mass/body weight ratios (n = 7–11 mice) (C), representative images of H&E-stained WAT and BAT sections (scale bar: 200 μm; n = 7–11 mice) (D), and mRNA levels of lipogenic (E and F) and lipolytic (G) genes in the WAT and BAT from DKO and WT mice upon chow (n = 7–11 mice). (H, I) Representative electron microscopy images (H) (abnormal mitochondria with irregular shape [asterisks], loss of cristae [empty arrowheads], or myelin figures [arrowheads]; magnification: 10,000×), and quantification of the structure of BAT (I) from DKO and WT mice upon HFD (n = 4–6 mice). (J) mRNA levels of thermogenic genes of the BAT from WT and DKO mice upon HFD (n = 5-6 mice). Data are represented as mean ± SEM. Student's *t* test. **p* <0.05, ***p* <0.01, *****p* <0.0001. *Acc1*, acetyl-CoA carboxylase 1; *Atgl*, adipose triglyceride lipase; BAT, brown adipose tissue; *C/Ebpa*, CCAAT/enhancer binding protein alpha; *Dgat1*, diacylglycerol O-acyltransferase 1; *Dgat2*, diacylglycerol O-acyltransferase 2; *Dio2*, deiodinase, iodothyronine, type II; DKO, *Fxr* and *Shp* double knockout; *Fasn*, fatty acid synthase; *Fxr*, farnesoid X receptor; HFD, high-fat diet; *Hsl*, hormone-sensitive lipase; H&E, hematoxylin and eosin; *Pgc1a*, peroxisome proliferative activated receptor, gamma, coactivator 1 alpha; *Pparg*, peroxisome proliferator activated receptor gamma; *Prdm16*, PR domain containing 16; *Scd1*, stearoyl-coenzyme A desaturase 1; *Shp*, small heterodimer; *Srebp1c*, sterol regulatory element binding protein 1c; TN, thermoneutrality; Ucp1, uncoupling protein 1; WAT, white adipose tissue; WT, wild-type.

alpha [*C/Ebpa*] and diacylglycerol O-acyltransferase 2 [*Dgat2*]) (Fig. 1C) and BAT (*C/Ebpa,* sterol regulatory element binding protein 1c [*Srebp1c*], diacylglycerol O-acyltransferase 1 [*Dgat1*], and *Dgat2*) (Fig. 1D). These data suggest a possibility of reduced lipogenesis in the DKO adipose tissues. Although we did find increased mRNA levels of stearoyl-coenzyme A desaturase 1 (SCD1) (Fig. 1C), a rate-limiting enzyme for the synthesis of unsaturated fatty acids,[21] in the DKO WAT, no alteration was observed in the degrees of unsaturation as measured with Raman spectroscopy compared with WT mice (Fig. S2C). Further, we investigated and found that the response to β-adrenergic stimulation with isoproterenol was dampened in DKO mice compared with that in WT mice (Fig. 1E). We also found lower transcript levels of hormone-sensitive lipase (*Hsl*) and adipose triglyceride lipase (*Atgl*) in the WAT and BAT, respectively (Fig. 1F,G), which corroborates with lower stimulated lipolysis in DKO mice.

As mitochondrially rich BAT promotes heat production and is implicated in BA-mediated fat burning,[12] we examined gene expression and mitochondrial activity and continually monitored the body temperature of DKO and WT mice. Intriguingly, DKO mice exhibited decreased expression of thermogenic genes PR domain containing 16 (*Prdm16*) and *Ucp1* (Fig. 2A). We validated the reduction in UCP1 protein levels (Fig. 2B) and activities of citrate synthase as well as oxidative phosphorylation (OXPHOS) enzyme complexes III and IV albeit an increase in complex I (Fig. 2C). Consistently, DKO BAT displayed dramatically lower mitochondrial respiration including state III, coupled, and uncoupled/leak respiration (Fig. 2D,E). However, the mtDNA copy number, a surrogate indicator of mitochondrial numbers, was comparable between DKO and WT mice (Fig. 2F), suggesting that DKO mice do not have less mitochondria. We also tested whether BA overload in DKO caused cell death in the brown fat depots by terminal deoxynucleotidyl transferase dUTP nick end labeling (TUNEL) staining and found no positive cells (Fig. S2D), indicating the absence of apoptosis. Instead, coherent with poor mitochondrial function, DKO mice exhibited lower body temperature than WT mice during the daytime; however, the activity-induced increase in body temperature at night was unaffected (Fig. 2G).

Next, we examined these adipose depots after challenging DKO and WT mice for 8 weeks with a 45% HFD. DKO mice maintained lower fat mass (Fig. S2E) and smaller adipocyte size (Fig. S2F,G) in both the fat depots compared with WT mice upon HFD challenge. This result is in line with significant reductions in the expression of key lipogenic genes including peroxisome proliferator activated receptor gamma (*Pparg*), *C/Ebpa*, *Srebp1c*, acetyl-CoA carboxylase 1 (*Acc1*), fatty acid synthase (*Fasn*), *Scd1*, *Dgat1*, and *Dgat2* in the DKO BAT (Fig. S2I). However, lipogenic gene expression profile was not different between the two genotypes in the WAT except for lower levels of *Dgat2* (Fig. S2H). DKO WAT displayed an increase but DKO BAT showed a decrease in transcript levels of *Atgl* compared with WT mice (Fig. S2J). Although we did not find overt difference in mitochondrial ultrastructure using electron microscopy (Fig. 2H), we discovered lower expression of thermogenic genes *Prdm16*, *Pgc1a*, *Dio2*, and *Ucp1* (Fig. 2I) and a reduction in UCP1 protein levels (Fig. 2J) in DKO *vs*. WT mice under HFD. In addition, mtDNA copy number was lower in the DKO BAT than in the WT BAT (Fig. 2K). We also confirmed that these effects in HFD are not caused by cell death, as we observed negligible TUNEL staining of BAT (Fig. S2K). These results suggest that BA excess can impair expression of lipogenic genes and decrease thermogenic function in the adipocytes irrespective of the diet.

Thermoneutral housing is sufficient to increase brown fat mass during cholestasis

To confirm the brown adipose mitochondrial dysfunction in cholestatic DKO mice, we housed both WT and DKO mice at TN (30 °C), which excludes the thermogenic effect of the BAT.[19] The decreases in mRNA levels of *Prdm16* and *Ucp1* noted in the DKO BAT compared with that in the WT BAT at RT (Fig. 2A) were abolished at TN (Fig. 3A). In addition, UCP1 protein levels at TN were similar between the WT and DKO BAT (Fig. 3B). Despite a slightly smaller adipocyte size (Fig. 3D and Fig. S3A), the brown fat mass at TN was comparable between WT and DKO mice (Fig. 3C), which correlated well with the similar transcription profile of key lipogenic and lipase genes (Fig. 3F,G). These results indicate that the ineffective brown fat function may, in part, protect DKO mice against obesity, which is in line with previous studies that adipose-specific mitochondrial dysregulation causes fat loss.[22,23] Although thermoneutral housing enhanced *C/Ebpa* transcript expression in the DKO WAT compared with that in WT and altered other genes in the lipogenic pathways (Figs. 1C and 3E), DKO mice still exhibited reduced white fat mass (Fig. 3C) and smaller adipocyte size (Fig. 3D and Fig. S3A).

Next, we challenged DKO and WT mice housed at 30 °C with an HFD for 8 weeks. This double hit led to a dramatic decrease in the ratio of normal mitochondria in the DKO BAT, with the majority of them revealing abnormal ultrastructure with irregular shape, loss of cristae, or presence of myelin figures (Fig. 3H,I), all of which indicate mitochondrial damage or degeneration.[24,25] Under thermoneutral conditions, HFD-fed DKO mice displayed similar levels of *Prdm16* and *Pgc1a* but lower expression of *Dio2* and *Ucp1* in the BAT compared with HFD-fed WT mice when housed at TN (Fig. 3J). Nonetheless, at TN, DKO mice gained a similar percentage of body weight as WT mice in response to HFD (Fig. S3B), unlike poor weight gain seen in DKO mice under normal housing conditions. Notably, DKO and WT mice exhibited comparable BAT mass at TN, but WAT mass was still lower in DKO mice than in WT mice (Fig. S3C). The decrease in WAT adipocyte size was prominent and maintained in HFD-fed DKO mice housed at TN (Fig. S3D,E), despite induced expression of lipogenic genes in DKO mice compared with that in WT mice (Fig. S3F). By contrast, thermoneutral housing was sufficient to increase brown adipocyte size (Fig. 3D,E) and led to comparable expression of lipogenic genes *Pparg*, *C/Ebpa, Srebp1c*, and *Dgat1* in the BAT of HFD-fed DKO *vs*. HFD-fed WT mice (Fig. S3G). DKO WAT at TN showed expression of lipases similar to that seen at RT (Figs. S2J and S3H), whereas the reductions in *Atgl* and *Hsl* mRNA levels in DKO BAT were abrogated at TN (Figs. S2J and S3H). These findings indicate that WT and DKO BAT are comparable with each other under TN conditions.

DDC-fed mice mimic the brown adipose dysfunction phenotypes in DKO mice

FXR and SHP are implicated in lipid metabolism, and particularly, FXR has been shown to regulate adipose tissue lipid accumulation.[26–28] Therefore, to overcome the caveat of *Fxr* and *Shp* deletion in DKO mice, we examined a chronic DDC-induced model of cholestasis in WT mice with intact FXR and SHP expression. As expected, DDC diet led to elevated levels of circulating BAs (Fig. S4A), liver injury indicated by histological alterations (Fig. S4B), and raised serum concentrations of liver enzymes

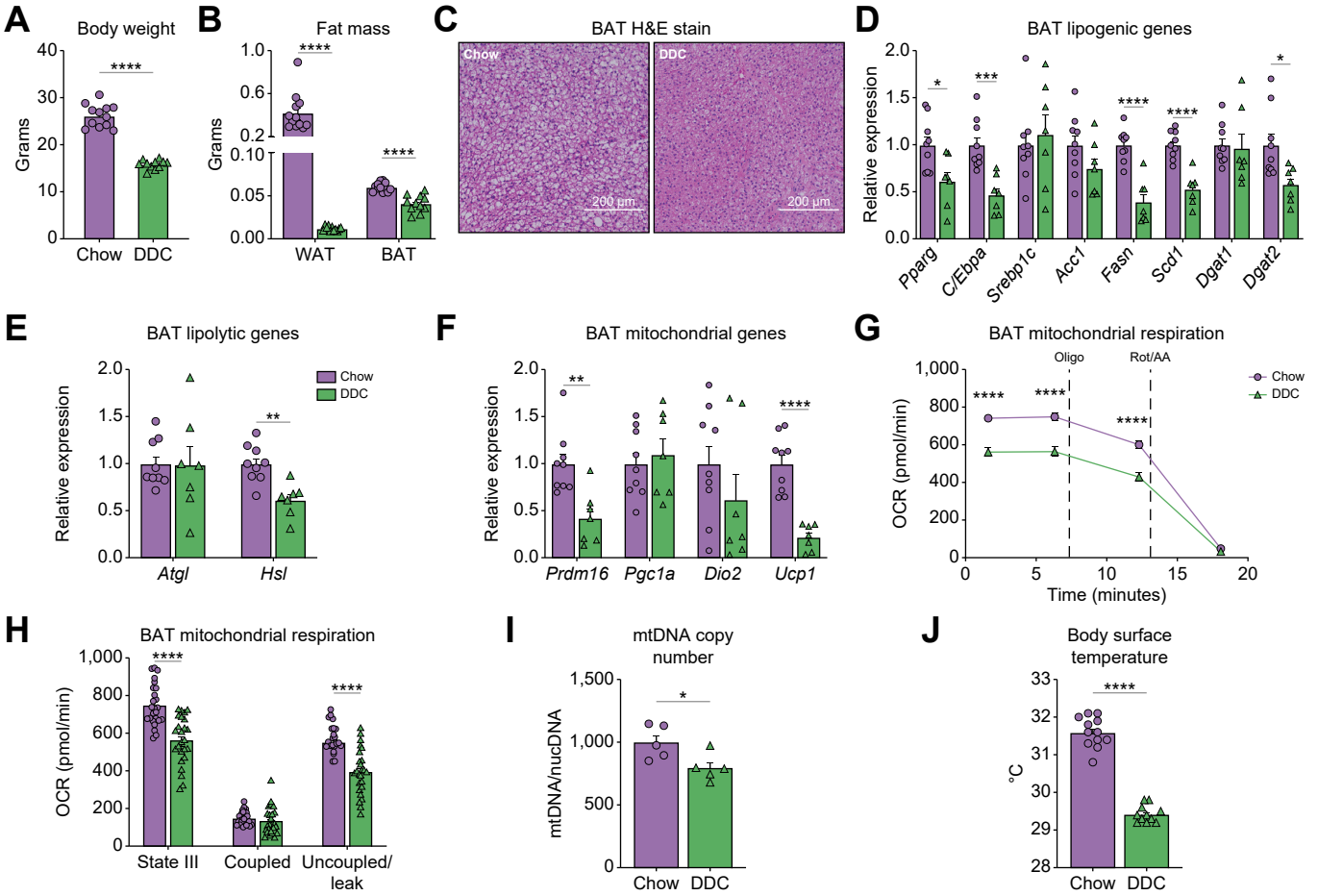

Fig. 4. Cholestatic DDC-fed mice show attenuated BAT mitochondrial function and fat loss. (A–F) Body weight (n = 11–12 mice) (A), white and brown fat mass (n = 11–12 mice) (B), representative images of H&E-stained BAT sections (scale bar: 200 µm) (n = 8–10 mice) (C), transcript levels of lipogenic (D), lipolytic (E), and thermogenic (F) genes in the BAT of DDC- and chow-fed WT mice (n = 7–9 mice). (G, H) Traces (G) and quantification (H) of OCR of BAT-isolated mitochondria from DDC- and chow-fed WT mice. OCR at state III and in the presence of Oligo or Rot/AA (n = 25 wells per group isolated from BAT of 9 mice). (I) Relative mtDNA content of BAT from DDC- and chow-fed WT mice (n = 5 mice). (J) Body surface temperature of DDC- and chow-fed WT mice during daytime (n = 11–12 mice). Data are represented as mean ± SEM. Differences between two groups were analysed using Student's *t* test, and multiple-group comparisons were analysed using a two-way ANOVA with a Fisher's LSD *post hoc* test. **p* <0.05, ***p* <0.01, ****p* <0.001, *****p* <0.0001. *Acc1*, acetyl-CoA carboxylase 1; *Atgl*, adipose triglyceride lipase; BAT, brown adipose tissue; *C/Ebpa*, CCAAT/enhancer binding protein alpha; DDC, 3,5-diethoxycarbonyl-1,4-dihydrocollidine; *Dgat1*, diacylglycerol O-acyltransferase 1; *Dgat2*, diacylglycerol O-acyltransferase 2; *Dio2*, deiodinase, iodothyronine, type II; *Fasn*, fatty acid synthase; *Hsl*, hormone-sensitive lipase; H&E, hematoxylin and eosin; LSD, least significant difference; mtDNA, mitochondrial DNA; OCR, oxygen consumption rate; Oligo, oligomycin; *Pgc1a*, peroxisome proliferative activated receptor, gamma, coactivator 1 alpha; *Pparg*, peroxisome proliferator activated receptor gamma; *Prdm16*, PR domain containing 16; Rot/AA, rotenone and antimycin A; *Scd1*, stearoyl-coenzyme A desaturase 1; *Srebp1c*, sterol regulatory element binding protein 1c; Ucp1, uncoupling protein 1; WAT, white adipose tissue; WT, wild-type.

aspartate transaminase and alanine transaminase (Fig. S4C) in WT mice. We also observed that DDC challenge led to a lower body weight (Fig. 4A) as anticipated, which was accompanied by the loss of WAT mass (Fig. 4B), and a decrease in brown fat mass (Fig. 4B) and adipocyte size (Fig. 4C and Fig. S4D). The weight loss with DDC was drastic at 2 weeks and then stabilizes; therefore, we examined daily food intake using a CLAMS. Food intake was comparable between DDC- and chow-fed mice (Fig. S4E). Energy expenditure during the day remained unaltered, but the active nighttime energy expenditure was increased despite reduced physical activity in DDC-fed cholestatic mice (Fig. S4F,G).

Upon further analysis, we found that brown fat from DDC-fed mice phenocopied many aspects of the BAT from DKO mice, including the reduction in lipogenic genes *C/Ebpa* and *Dgat2* along with *Pparg*, *Fasn*, and *Scd1*, which was unique to the DDC diet (Figs. 1D and 4D). Remarkably, brown fat from DDC-fed WT mice also recapitulated the reductions in thermogenic genes *Prdm16* and *Ucp1* (Figs. 2A and 4F). We also found reduced mitochondrial respiration, including state III and uncoupled/leak respiration (Fig. 4G,H), and lower mtDNA copy number (Fig. 4I) in DDC-fed WT BAT. In line with these changes, DDC-fed mice exhibited lower body temperature during the light phase similarly to cholestatic DKO mice (Figs. 2G and 4J). In addition, we confirmed that the reductions in thermogenic genes and mitochondrial defect were not secondary to cell death as measured by TUNEL staining (Fig. S4H). These results demonstrate that chronic cholestasis causes defects in brown adipose function, leading to poor thermogenesis and fat loss.

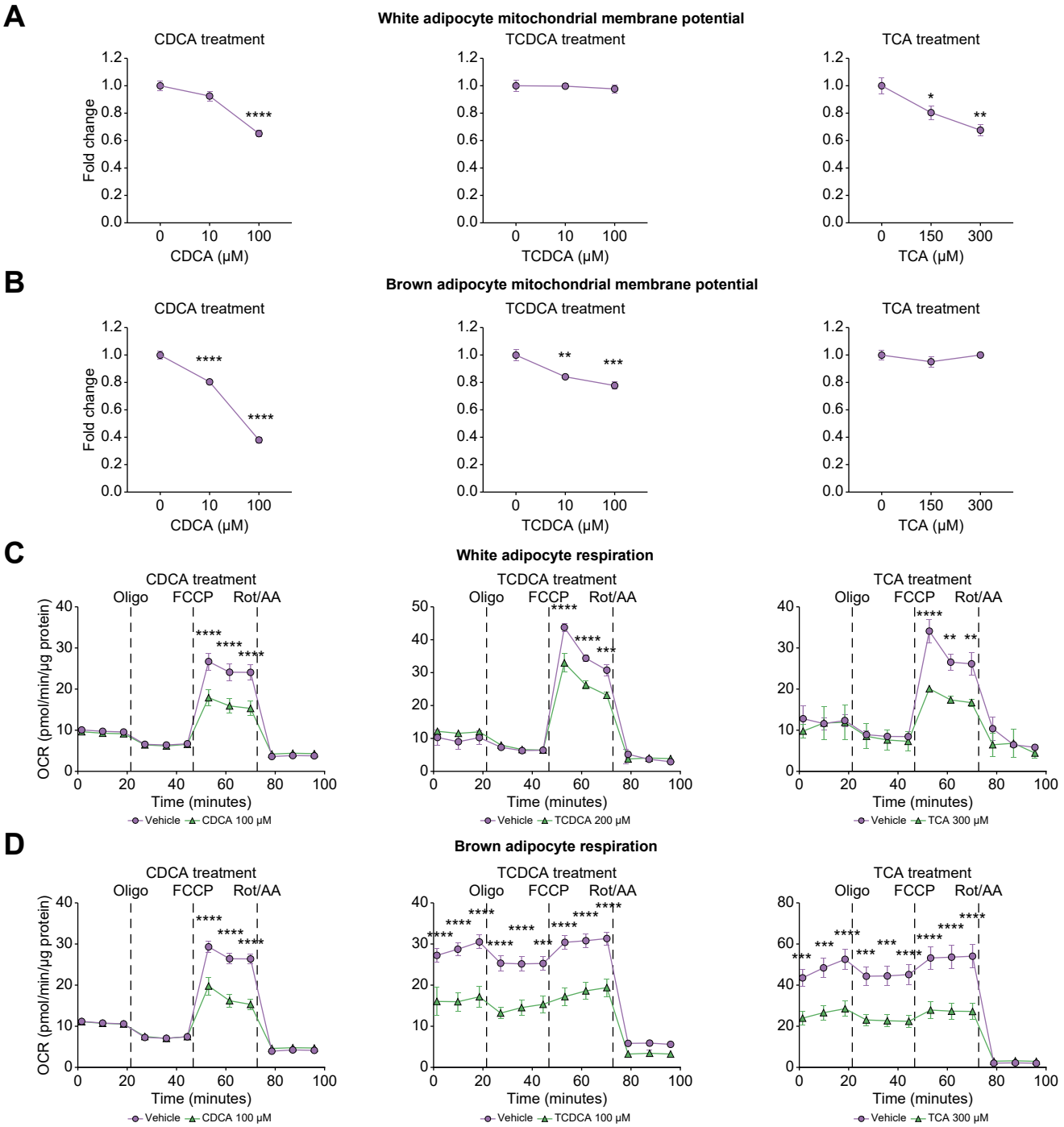

Fig. 5. Pathological levels of BAs result in adipocyte mitochondrial dysfunction *in vitro*. Primary adipocyte cultures were isolated from WAT and BAT of 5–6 mice, and n = 4–5 wells per treatment were used for analysis. (A, B) Mitochondrial membrane potential of white (A) and brown (B) adipocytes upon different concentrations of CDCA, TCDCA, or TCA treatment for 24 h. (C, D) Traces of OCR of CDCA/TCDCA/TCA-treated white (C) and brown (D) adipocytes. OCR at basal and in the presence of Oligo, FCCP, or Rot/AA. Data are represented as mean ± SEM. Differences between multiple groups were analysed using a one-way or two-way ANOVA with a Fisher's LSD *post hoc* test. *p <0.05, **p <0.01, ***p <0.001, ****p <0.0001. BA, bile acid; BAT, brown adipose tissue; CDCA, chenodeoxycholic acid; FCCP, carbonyl cyanide-4-(trifluoromethoxy) phenylhydrazone; LSD, least significant difference; OCR, oxygen consumption rate; Oligo, oligomycin; Rot/AA, rotenone and antimycin A; TCA, taurocholic acid; TCDCA, taurochenodeoxycholic acid; WAT, white adipose tissue.

Pathological BA concentrations are sufficient to cause mitochondrial dysfunction in adipocytes

To determine the cell autonomous effect of BAs, we treated differentiated primary adipocytes derived from either WAT or BAT with pathological concentrations of primary BAs chenodeoxycholic acid (CDCA), taurochenodeoxycholic acid (TCDCA), or taurocholic acid (TCA).[29] Excess CDCA, TCDCA, and TCA resulted in a general decline in mitochondrial membrane

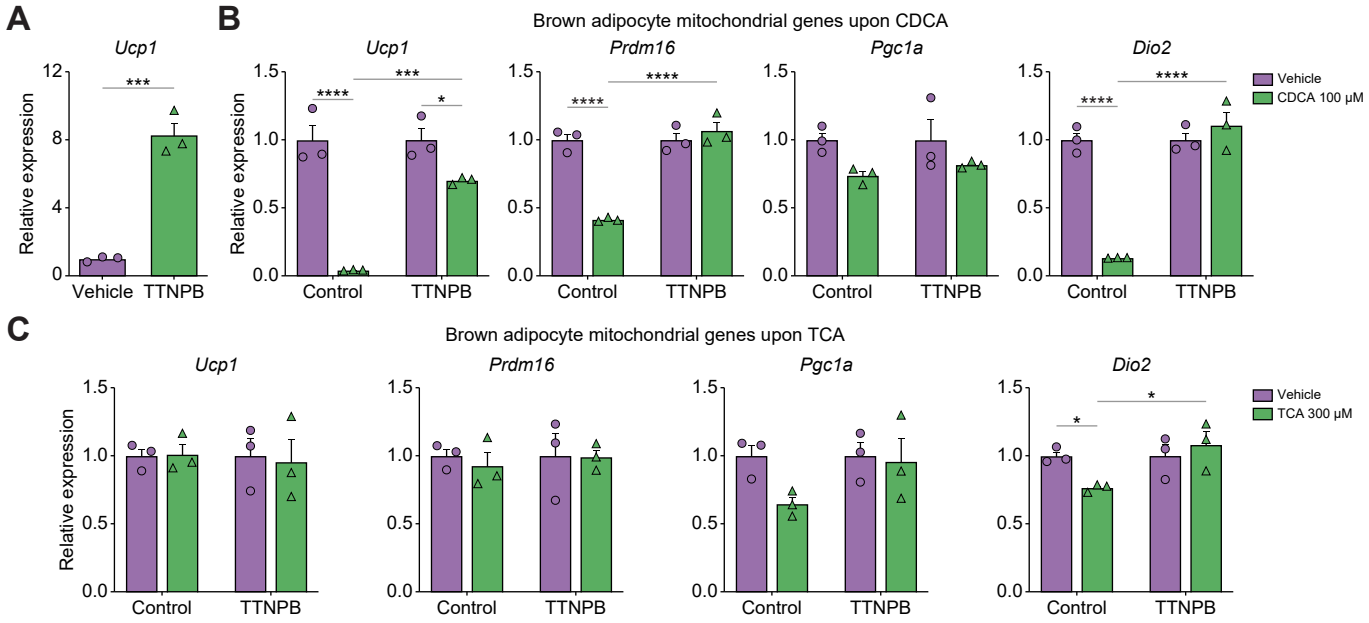

Fig. 6. UCP1 activation rescues BA overload-induced reductions in the expression of thermogenic genes in brown adipocytes. Primary adipocyte cultures were isolated from BAT of 6 mice, and n = 3 wells per treatment were used for analysis. (A) *Ucp1* mRNA levels in brown adipocytes upon TTNPB (1 nM) treatment for 48 h. (B, C) mRNA levels of genes responsible for mitochondrial function in differentiated brown adipocytes with or without TTNPB (1 nM) administration for 24 h followed by another 24-h treatment of CDCA (100 μM) (B) or TCA (300 μM) (C). Data are represented as mean ± SEM. Differences between two groups were analysed using Student's *t* test, and multiple-group comparisons were analysed using a one-way ANOVA with a Fisher's LSD *post hoc* test. **p* <0.05, ****p* <0.001, *****p* <0.0001. BA, bile acid; BAT, brown adipose tissue; CDCA, chenodeoxycholic acid; *Dio2*, deiodinase, iodothyronine, type II; LSD, least significant difference; *Pgc1a*, peroxisome proliferative activated receptor, gamma, coactivator 1 alpha; *Prdm16*, PR domain containing 16; TCA, taurocholic acid; Ucp1, uncoupling protein 1.

potential (Fig. 5A,B) and respiration (Fig. 5C,D and Fig. S5A,B) without affecting adipocyte viability (Fig. S5C). This result indicates that BAs regulate adipocyte mitochondrial function in a concentration-dependent manner. Elevated BAs lowered carbonyl cyanide-4-(trifluoromethoxy) phenylhydrazone (FCCP)-induced maximal respiration compared to vehicle-treated adipocytes (Fig. 5C,D and Fig. S5A,B). Thus, BAs can reduce the spare respiratory capacity of the mitochondria, which is important to keep up with ATP demands of a cell. Further, TCDCA or TCA treatment resulted in lower basal and uncoupled/leak respiration (Fig. 5D and Fig. S5A,B), indicative of defective uncoupling in brown adipocytes.

To probe how BAs were altering mitochondria in adipocytes, we examined the literature to identify if there are putative genes that could transport BAs into adipocytes. We identified a subset of four possible transporters, namely solute carrier organic anion transporter family, member 1A6 (*Slco1a6*), solute carrier organic anion transporter family, member 1B2 (*Slco1b2*), solute carrier family 51, alpha subunit (*Slc51a*), and solute carrier family 51, beta subunit (*Slc51b*), that may transport BAs from the systemic circulation into the adipocytes. We validated their transcript expression in differentiated and undifferentiated primary adipocytes derived from either brown or white adipose depots. In white adipocytes, the expression profile of these transporters was maintained irrespective of the differentiation status except for a decrease in *Slc51a* post differentiation (Fig. S6A). We also confirmed the expression of human orthologues of *SLC51A* and *SLC51B* in human white fat depot (Fig. S6C). Intriguingly, however, the expression of *Slco1a6*, *Slco1b2,* and *Slc51b* were all induced upon differentiation specifically in brown adipocyte cultures (Fig. S6B), denoting the possibility of BA transport into mature brown adipocytes.

BA-induced suppression of thermogenic genes in brown adipocytes can be rescued by the activation of UCP1

In addition to mitochondrial activity, we also examined the expression of genes regulating thermogenesis and found that CDCA overload drastically reduced the expression of *Ucp1*, *Prdm16*, and *Dio2* transcripts in brown adipocytes (Fig. 6B), whereas in white adipocytes, we saw reductions in *Pgc1a*, *Dio2*, and carnitine palmitoyltransferase 1A, liver (*Cpt1a*) transcript levels (Fig. S7). As BAs are endogenous ligands for FXR and TGR5, we examined whether pharmacological activation of FXR[30] and/or TGR5[31] mimic the BA-mediated reductions of thermogenic genes. We found FXR agonist GW4064 suppressed *Prdm16* but induced *Dio2* (Fig. S8). In contrast, TGR5 activation induced the expression of *Ucp1, Prdm16, Pgc1a,* and *Dio2* as expected (Fig. S8). Finally, GW4064 in combination with INT-777 was able to dampen the induction of many of the thermogenic genes (Fig. S8). Overall, neither GW4064 nor INT-777 was able to fully recapitulate the CDCA-mediated reduction of all the analysed thermogenic genes.

Nonetheless, reduction of these genes was also noted in the cholestatic animal models, DKO and DDC-fed mice, highlighting the relevance of CDCA in mediating these defects. However, TCA overload reduced *Dio2* gene expression only in brown adipocytes

Table 1. Comparison summary between primary adipocyte cultures upon BA treatment, DKO, DDC-fed, and *Ucp1* KO mice housed at room temperature.

Parameter	BA-treated adipocytes	DKO mice	DDC-fed mice	*Ucp1* KO mice
Body weight	ND	↓	↓	↓,[41] NS[39]
WAT mass	ND	↓	↓	↓[38,39,41]
BAT mass	ND	↓	↓	NS[38,39]
BAT mitochondrial function	↓	↓	↓	↓[40]
Ucp1 levels	↓	↓	↓	↓[38–41]
Thermoregulation	ND	↓	↓	↓[38,39]
Skeletal muscle mitochondrial function	ND	↑[16]	ND	↑[41–43]
Energy expenditure	ND	↑[16]	↑	↑[41,42]

BA, bile acid; BAT, brown adipose tissue; DDC, 3,5-diethoxycarbonyl-1,4-dihydrocollidine; DKO, *Fxr* and *Shp* double knockout; Fxr, farnesoid X receptor; KO, knockout; ND, not determined; NS, not significant; *Shp*, small heterodimer; Ucp1, uncoupling protein 1; WAT, white adipose tissue.

(Fig. 6C and Fig. S7). The varied responses to different BA species in adipocytes from both fat depots suggest that the composition of the BA pool can also influence the outcome of mitochondrial function distinctly. Finally, we investigated whether the pharmacological activator of UCP1, TTNPB,[32,33] can alleviate some of these defects in the brown adipocytes. As previously shown, TTNPB dramatically upregulated *Ucp1* mRNA levels (Fig. 6A). Of note, the TTNPB treatment was sufficient to alleviate CDCA-mediated decreases in the transcript levels of *Prdm16* and *Dio2*, and TCA-induced reductions in the expression of *Dio2* (Fig. 6B,C). This result suggests that maintaining *Ucp1* mRNA during cholestasis is beneficial to maintain the thermogenic gene profile of brown adipocyte function.

Discussion

Several liver diseases result in weight and fat loss,[2–5] but the mechanisms underlying this fat loss remain unclear. Elevated circulating BA levels are observed in liver diseases[1] and are associated with fat burning.[2–5] In this study, we investigated the impact of chronic cholestatic disease on the adipose tissue function using two mouse models. We demonstrate that pathological BA concentrations are sufficient to cause mitochondrial dysfunction, poor thermoregulation, and fat loss.

Although a caveat of the DKO model of cholestasis is that it is a global knockout of *Fxr* and *Shp,* it captures an increase in BA mixture rather than an increase in a single type of BAs and mimics pediatric cholestasis.[14] Importantly, the individual *Fxr* and *Shp* knockouts do not accumulate pathological BAs to the extent of what is observed in the clinical setting.[11,14] To overcome this caveat and to tease apart the BA effect, we also performed *in vivo* studies using a DDC-induced cholestasis mouse model and *in vitro* studies using primary adipocyte cultures from white and brown adipose with intact FXR and SHP signalling.

Consistent with previous findings that BAs can promote brown adipose activity by activating TGR5-cAMP-DIO2 signalling pathway,[6,7] we observed that short-term administration of BAs induced *Dio2* and *Pgc1a* transcript expression (Fig. S1). However, during chronic cholestasis, BA concentrations can elevate to hundreds of micromolar, which in turn impairs BAT mitochondrial function, leading to poor thermoregulation as observed in both DKO and DDC-fed cholestatic mice. This is surprising because we had previously found enhanced mitochondrial function in DKO skeletal muscle.[16] These results demonstrate tissue-specific effects of BA overload such that skeletal muscle activity is increased but the brown fat mitochondrial function is compromised. Neither *Fxr* nor *Shp* deletion alters the basal BAT thermogenic gene expression,[34,35] indicating that this effect is secondary to BA overload. We also examined for cell death in the BAT and did not find the evidence for it (Fig. S2D,K and S4H). Importantly, heat generated by brown fat[36] was hampered in both cholestatic mouse models, and they displayed lower body temperature (Figs. 2G and 4J).

To evaluate the direct consequence of BAs on adipocytes, we examined primary adipocyte cultures obtained from white or brown fat depot. Adipocytes treated with pathological BA concentrations as observed in clinical cholestasis[29] were viable (Fig. S5C) but revealed poor mitochondrial function (Fig. 5A–D, 6B,C, Fig. S5A,B, and S7). Such impairments in mitochondrial respiration, increased mitochondrial permeability, and cellular injury have also been noted in hepatocytes[9,37] and cardiomyocytes[10,11] upon high BA levels.

Agonistic activation of FXR or TGR5 did not recapitulate the suppression of thermogenic genes subsequent to high concentrations of CDCA (Fig. S8). TGR5 activation induced them, whereas FXR agonist reduced only *Prdm16* transcript in brown adipocytes. However, cotreatment led to inhibition of TGR5 effects when FXR was activated, indicating a complex interplay of these two signalling maybe involved in brown adipocytes upon pathological BA exposure.

Of note, UCP1 suppression in cholestasis was conserved in mice and adipocyte cultures. Intriguingly, *Ucp1* deficiency or mitochondrial dysfunction has been linked to fat loss and resistance to diet-induced obesity.[38–41] It is postulated that skeletal muscle-based thermogenesis may compensate for defective heat production in the BAT of *Ucp1* knockout mice.[41–43] Thermogenesis is negated under TN (30 °C), and *Ucp1*-deficient mice gain weight and lose their resistance to diet-induced obesity[38,44] when housed at 30 °C. Our findings reveal that DKO and DDC-fed cholestatic mice exhibit overlapping phenotypes with *Ucp1* knockout mice, including reduced *Ucp1* levels, fat loss, impaired BAT mitochondrial function, and dysregulated thermogenesis (Table 1). Notably, thermoneutral housing reversed the reductions in body weight gain and brown fat mass of DKO mice (Fig. 3C and Fig. S3B,C), highlighting the reduction of UCP1-mediated brown fat thermogenesis in cholestasis. More importantly, activating UCP1 is sufficient to recover the expression of thermogenic genes *Prdm16* and/or *Dio2* (Fig. 6B,C). Our findings uncover that BA excess can lead to mitochondrial defect in the BAT and may explain these clinical presentations of fat loss[2–5] and hypothermia[45–47] that have been associated in patients with cholestasis.[1]

Abbreviations

Acc1, acetyl-CoA carboxylase 1; *Atgl*, adipose triglyceride lipase; BA, bile acid; BAT, brown adipose tissue; *C/Ebpa*, CCAAT/enhancer binding protein alpha; CA, cholic acid; CDCA, chenodeoxycholic acid; CLAMS, Comprehensive Laboratory Animal Monitoring System; *Cpt1a*, carnitine palmitoyltransferase 1A, liver; DDC, 3,5-diethoxycarbonyl-1,4-dihydrocollidine; *Dgat1*, diacylglycerol O-acyltransferase 1; *Dgat2*, diacylglycerol O-acyltransferase 2; *Dio2*, deiodinase, iodothyronine, type II; DKO, *Fxr* and *Shp* double knockout; *Fasn*, fatty acid synthase; FCCP, carbonyl cyanide-4-(trifluoromethoxy) phenylhydrazone; FFA, free fatty acid; *Fxr*, farnesoid X receptor; HFD, high fat diet; *Hsl*, hormone-sensitive lipase; IRB, institutional review board; LSD, least significant difference; mtDNA, mitochondrial DNA; nucDNA, nuclear DNA; ND, not determined; NS, not significant; OCR, oxygen consumption rate; Oligo, oligomycin; OXPHOS, oxidative phosphorylation; *Pgc1a*, peroxisome proliferative activated receptor, gamma, coactivator 1 alpha; *Pparg*, peroxisome proliferator activated receptor gamma; *Prdm16*, PR domain containing 16; Rot/AA, rotenone and antimycin A; RT, room temperature; *Scd1*, stearoyl-coenzyme A desaturase 1; *Shp*, small heterodimer partner; *Slc51a*, solute carrier family 51, alpha subunit; *Slc51b*, solute carrier family 51, beta subunit; *Slco1a6*, solute carrier organic anion transporter family, member 1A6; *Slco1b2*, solute carrier organic anion transporter family, member 1B2; *Srebp1c*, sterol regulatory element binding protein 1c; TCA, taurocholic acid; TCDCA, taurochenodeoxycholic acid; TGR5, G protein-coupled bile acid receptor 1; TN, thermoneutrality; TUNEL, terminal deoxynucleotidyl transferase dUTP nick end labeling; Ucp1, uncoupling protein 1; WAT, white adipose tissue; WT, wild-type; ZT, zeitgeber time.

Financial support

This work was supported by start-up funds from the University of Illinois Urbana-Champaign (SA), R01 DK113080 (SA), R01 DK130317 (SA), and Cancer Center at Illinois Planning Grant and Seed grant (SA), and NIH/NCI R01CA241618 (to institution [SAB]).

Conflicts of interest

SAB reports consulting fees and stock from LiveBx, LLC. WZ reports Early Career Investigator Award from Kern Lipid Conference to attend Kern Lipid Conference 2022. MB reports Diversity Travel Award from the Obesity Society to attend Obesity Week 2022. The other authors declare no conflicts of interest that pertain to this work.

Please refer to the accompanying ICMJE disclosure forms for further details.

Authors' contributions

Conceived and designed research: WZ, PV, SA. Supplied human adipose samples: BMR, MTG, MB. Performed experiments: WZ, PV, CZ, YL, RR, SA. Were responsible for Raman spectroscopy analysis: CZ, SAB. Analysed data: WZ, PV, CZ, YL, RR. Interpreted data: WZ, PV, CZ, YL, RR, SA. Drafted the manuscript: WZ, SA. Were involved in editing and revising the manuscript, and had final approval of the submitted and published versions: all authors.

Data availability statement

All data are in the main text and the Supplementary information.

Acknowledgements

The authors are grateful to Dr. Oludemilade Akinrotimi for her assistance with obtaining transmission electron microscopy samples for analysis, Mr. Shawn D'Souza for quantitative real-time PCR, and Dr. Lee-Jun Wong's laboratory at Baylor College of Medicine for mitochondrial complex activity analysis. We also thank Ms. Lou Ann Miller from the Biological Electron Microscopy core at Materials Research Laboratory, University of Illinois Urbana-Champaign, for performing transmission electron microscopy. We acknowledge the Microscopy Suite at the Beckman Institute, University of Illinois Urbana-Champaign, for the access to the Raman microspectrometer used in the study.

Supplementary data

Supplementary data to this article can be found online at https://doi.org/10.1016/j.jhepr.2023.100714.

References

Author names in bold designate shared co-first authorship.

[1] Neale G, Lewis B, Weaver V, Panveliwalla D. Serum bile acids in liver disease. Gut 1971;12:145–152.
[2] Squires JE, Celik N, Morris A, Soltys K, Mazariegos G, Shneider B, et al. Clinical variability after partial external biliary diversion in familial intrahepatic cholestasis 1 deficiency. J Pediatr Gastroenterol Nutr 2017;64:425–430.
[3] Beckett GJ, Dewhurst N, Finlayson ND, Percy-Robb IW. Weight loss in primary biliary cirrhosis. Gut 1980;21:734–737.
[4] Williamson KD, Chapman RW. Primary sclerosing cholangitis. Dig Dis 2014;32:438–445.
[5] Reyes H, Radrigan ME, Gonzalez MC, Latorre R, Ribalta J, Segovia N, et al. Steatorrhea in patients with intrahepatic cholestasis of pregnancy. Gastroenterology 1987;93:584–590.
[6] **Watanabe M**, **Houten SM**, Mataki C, Christoffolete MA, Kim BW, Sato H, et al. Bile acids induce energy expenditure by promoting intracellular thyroid hormone activation. Nature 2006;439:484–489.
[7] **Broeders EP**, **Nascimento EB**, Havekes B, Brans B, Roumans KH, Tailleux A, et al. The bile acid chenodeoxycholic acid increases human brown adipose tissue activity. Cell Metab 2015;22:418–426.
[8] Rolo AP, Oliveira PJ, Moreno AJ, Palmeira CM. Bile acids affect liver mitochondrial bioenergetics: possible relevance for cholestasis therapy. Toxicol Sci 2000;57:177–185.
[9] Yerushalmi B, Dahl R, Devereaux MW, Gumpricht E, Sokol RJ. Bile acid-induced rat hepatocyte apoptosis is inhibited by antioxidants and blockers of the mitochondrial permeability transition. Hepatology 2001;33:616–626.
[10] Ferreira M, Coxito PM, Sardão VA, Palmeira CM, Oliveira PJ. Bile acids are toxic for isolated cardiac mitochondria: a possible cause for hepatic-derived cardiomyopathies? Cardiovasc Toxicol 2005;5:63–73.
[11] **Desai MS**, **Mathur B**, Eblimit Z, Vasquez H, Taegtmeyer H, Karpen SJ, et al. Bile acid excess induces cardiomyopathy and metabolic dysfunctions in the heart. Hepatology 2017;65:189–201.
[12] Cohen P, Spiegelman BM. Cell biology of fat storage. Mol Biol Cel 2016;27:2523–2527.
[13] **Nguyen JT**, **Riessen R**, Zhang T, Kieffer C, Anakk S. Deletion of intestinal SHP impairs short-term response to cholic acid challenge in male mice. Endocrinology 2021;162:bqab063.
[14] Anakk S, Watanabe M, Ochsner SA, McKenna NJ, Finegold MJ, Moore DD. Combined deletion of *Fxr* and *Shp* in mice induces Cyp17a1 and results in juvenile onset cholestasis. J Clin Invest 2011;121:86–95.
[15] Mathur B, Arif W, Patton ME, Faiyaz R, Liu J, Yeh J, et al. Transcriptomic analysis across liver diseases reveals disease-modulating activation of constitutive androstane receptor in cholestasis. JHEP Rep 2020;2:100140.
[16] **Akinrotimi O**, **Riessen R**, VanDuyne P, Park JE, Lee YK, Wong LJ, et al. Small heterodimer partner deletion prevents hepatic steatosis and when combined with farnesoid X receptor loss protects against type 2 diabetes in mice. Hepatology 2017;66:1854–1865.
[17] Pose E, Sancho-Bru P, Coll M. 3,5-Diethoxycarbonyl-1,4-dihydrocollidine diet: a rodent model in cholestasis research. Methods Mol Biol 2019;1981:249–257.
[18] Robinson KN, Rowitz B, Oliphant UJ, Donovan SM, Teran-Garcia M. Larger omental adipocytes correlate with greater Fetuin-A reduction following sleeve gastrectomy. BMC Obes 2019;6:15.
[19] **Boutant M**, **Kulkarni SS**, Joffraud M, Ratajczak J, Valera-Alberni M, Combe R, et al. Mfn2 is critical for brown adipose tissue thermogenic function. EMBO J 2017;36:1543–1558.
[20] Mei J, Riedel N, Grittner U, Endres M, Banneke S, Emmrich JV. Body temperature measurement in mice during acute illness: implantable temperature transponder versus surface infrared thermometry. Sci Rep 2018;8:3526.
[21] Lodhi IJ, Wei X, Semenkovich CF. Lipoexpediency: de novo lipogenesis as a metabolic signal transmitter. Trends Endocrinol Metab 2011;22:1–8.

[22] Yang H, Wu JW, Wang SP, Severi I, Sartini L, Frizzell N, et al. Adipose-specific deficiency of fumarate hydratase in mice protects against obesity, hepatic steatosis, and insulin resistance. Diabetes 2016;65:3396–3409.
[23] Vernochet C, Damilano F, Mourier A, Bezy O, Mori MA, Smyth G, et al. Adipose tissue mitochondrial dysfunction triggers a lipodystrophic syndrome with insulin resistance, hepatosteatosis, and cardiovascular complications. FASEB J 2014;28:4408–4419.
[24] Le Beux Y, Hetenyi Jr G, Phillips MJ. Mitochondrial myelin-like figures: a non-specific reactive process of mitochondrial phospholipid membranes to several stimuli. Z Zellforsch Mikrosk Anat 1969;99:491–506.
[25] Sisková Z, Mahad DJ, Pudney C, Campbell G, Cadogan M, Asuni A, et al. Morphological and functional abnormalities in mitochondria associated with synaptic degeneration in prion disease. Am J Pathol 2010;177:1411–1421.
[26] Abdelkarim M, Caron S, Duhem C, Prawitt J, Dumont J, Lucas A, et al. The farnesoid X receptor regulates adipocyte differentiation and function by promoting peroxisome proliferator-activated receptor-γ and interfering with the Wnt/β-catenin pathways. J Biol Chem 2010;285:36759–36767.
[27] van Zutphen T, Stroeve JHM, Yang J, Bloks VW, Jurdzinski A, Roelofsen H, et al. FXR overexpression alters adipose tissue architecture in mice and limits its storage capacity leading to metabolic derangements. J Lipid Res 2019;60:1547–1561.
[28] Zhou W, Anakk S. Enterohepatic and non-canonical roles of farnesoid X receptor in controlling lipid and glucose metabolism. Mol Cel Endocrinol 2022;549:111616.
[29] Barnes S, Gallo GA, Trash DB, Morris JS. Diagnositic value of serum bile acid estimations in liver disease. J Clin Pathol 1975;28:506–509.
[30] Cariou B, van Harmelen K, Duran-Sandoval D, van Dijk TH, Grefhorst A, Abdelkarim M, et al. The farnesoid X receptor modulates adiposity and peripheral insulin sensitivity in mice. J Biol Chem 2006;281:11039–11049.
[31] Velazquez-Villegas LA, Perino A, Lemos V, Zietak M, Nomura M, Pols TWH, et al. TGR5 signalling promotes mitochondrial fission and beige remodelling of white adipose tissue. Nat Commun 2018;9:245.
[32] Jash S, Banerjee S, Lee MJ, Farmer SR, Puri V. CIDEA transcriptionally regulates UCP1 for britening and thermogenesis in human fat cells. iScience 2019;20:73–89.
[33] Keipert S, Jastroch M. Brite/beige fat and UCP1 – is it thermogenesis? Biochim Biophys Acta 2014;1837:1075–1082.
[34] **Zhang Y**, **Ge X**, Heemstra LA, Chen WD, Xu J, Smith JL, et al. Loss of FXR protects against diet-induced obesity and accelerates liver carcinogenesis in ob/ob mice. Mol Endocrinol 2012;26:272–280.
[35] Park YJ, Kim SC, Kim J, Anakk S, Lee JM, Tseng HT, et al. Dissociation of diabetes and obesity in mice lacking orphan nuclear receptor small heterodimer partner. J Lipid Res 2011;52:2234–2244.
[36] Blondin DP, Haman F. Shivering and nonshivering thermogenesis in skeletal muscles. Handb Clin Neurol 2018;156:153–173.
[37] Zhou W, Anakk S. Melancholé: the dark side of bile acids and its cellular consequences. Cell Mol Gastroenterol Hepatol 2022;13:1474–1476.
[38] Liu X, Rossmeisl M, McClaine J, Riachi M, Harper ME, Kozak LP. Paradoxical resistance to diet-induced obesity in UCP1-deficient mice. J Clin Invest 2003;111:399–407.
[39] **Enerbäck S**, **Jacobsson A**, **Simpson EM**, Guerra C, Yamashita H, Harper ME, et al. Mice lacking mitochondrial uncoupling protein are cold-sensitive but not obese. Nature 1997;387:90–94.
[40] **Kazak L**, **Chouchani ET**, Stavrovskaya IG, Lu GZ, Jedrychowski MP, Egan DF, et al. UCP1 deficiency causes brown fat respiratory chain depletion and sensitizes mitochondria to calcium overload-induced dysfunction. Proc Natl Acad Sci USA 2017;114:7981–7986.
[41] Bal NC, Singh S, Reis FCG, Maurya SK, Pani S, Rowland LA, et al. Both brown adipose tissue and skeletal muscle thermogenesis processes are activated during mild to severe cold adaptation in mice. J Biol Chem 2017;292:16616–16625.
[42] Shabalina IG, Hoeks J, Kramarova TV, Schrauwen P, Cannon B, Nedergaard J. Cold tolerance of UCP1-ablated mice: a skeletal muscle mitochondria switch toward lipid oxidation with marked UCP3 up-regulation not associated with increased basal, fatty acid- or ROS-induced uncoupling or enhanced GDP effects. Biochim Biophys Acta 2010;1797:968–980.
[43] Rowland LA, Bal NC, Kozak LP, Periasamy M. Uncoupling protein 1 and sarcolipin are required to maintain optimal thermogenesis, and loss of both systems compromises survival of mice under cold stress. J Biol Chem 2015;290:12282–12289.
[44] Feldmann HM, Golozoubova V, Cannon B, Nedergaard J. UCP1 ablation induces obesity and abolishes diet-induced thermogenesis in mice exempt from thermal stress by living at thermoneutrality. Cel Metab 2009;9:203–209.
[45] Gordon Jr AM. Causes of hypothermia. Arch Intern Med 1980;140:580.
[46] Gayed NM. Hypothermia associated with terminal liver failure. Am J Med 1987;83:808.
[47] Senadhi V. Recurrent hypothermia and hypoglycemia as the initial presentation of hepatitis C. Clin Pract 2011;1:e18.